Synthesis and Thermal Properties of Polystyrene/Montmorillonite Nanocomposites by γ-Ray Radiation Polymerization

Wei-An Zhang,[1] Xiao-Feng Shen,[2] Ming-Fei Liu,[1] Yue-E Fang[1]

[1]*Department of Polymer Science and Engineering, University of Science and Technology of China, Hefei, Anhui 230026, China*
[2]*Department of Chemistry, Anhui University, Hefei, Anhui 230039, China*

Received 26 November 2002; accepted 8 March 2003

ABSTRACT: Polystyrene/montmorillonite nanocomposites were prepared by γ-ray radiation polymerization. X-ray diffraction and high-resolution transmission electron microscopy confirmed that polystyrene (PS) could be easily inserted between the sheets of montmorillonite (MMT) to form intercalated nanocomposites. In these PS/MMT nanocomposites, the distance between the sheets of MMT was barely influenced by varying the content of the MMT. Thermal stabilities of the samples were studied by thermal gravimetric analysis and differential scanning calorimetry. The glass-transition temperature of PS/MMT nanocomposites was obviously higher than that of the pure PS. © 2003 Wiley Periodicals, Inc. J Appl Polym Sci 90: 1692–1696, 2003

Key words: polystyrene; nanocomposites; montmorillonite; γ-ray radiation; glass transition

INTRODUCTION

In recent years, polymer/clay nanocomposites have been extensively studied in many fields.[1–3] Nanocomposites are a new class of composites that are particle-filled polymers for which at least one dimension of the dispersed particles is in the nanometer range.[4,5] Polymer/clay composites can be called nanocomposites because the one dimension of clay is in the nanometer range. Compared with pure polymer or conventional composites, polymer/clay nanocomposites frequently exhibit unexpectedly improved mechanical, thermal, optical, and gas barrier properties derived from the nanometer-size particles obtained by dispersion.[6,7] Such polymer/clay nanocomposites were first reported by a Toyota research group.[8,9] Since then, many investigations have been conducted in this field and many polymer/clay nanocomposites have been synthesized, including those prepared by using, for example, the polymers polypropylene,[10] polycaprolactone,[11] poly(ethylene oxide),[12] polyamide,[13] polyimide,[14] epoxy,[15] polylactide,[16] poly(dimethylsiloxane),[17] and poly(styrene-*b*-butadiene).[18]

Currently, several methods have been considered in the preparation of polymer/clay nanocomposites, which include four main processes: exfoliation–adsorption, melt intercalation, template synthesis,[10] and *in situ* intercalative polymerization such as bulk, emulsion, or solution polymerization, although common to all processes is that they are all physical or initiated by chemical means.

The purpose of this study was to exhibit the synthesis of polystyrene/montmorillonite (PS/MMT) nanocomposites initiated by γ-ray radiation. Current literature does not report of polymer/clay nanocomposites prepared by γ-ray radiation.

EXPERIMENTAL

Materials

Styrene was purified by distillation at 10 mmHg to remove inhibitor and stored at −10°C before polymerization. Cetyltrimethylammonium bromide (CTAB) was purchased from Shanghai Chemical Reagents Co. (China). The Na^+–montmorillonite (Na–MMT), a most commonly used layered silicate clay, with a cation-exchange capacity (CEC) value of about 100 mmol/100 g (Ling An Chemicals Co. Ltd., Hangzhou, China), was used with further purification. The CEC was measured by the Co(II) procedure.[19]

Preparation of organophilic MMT

Organophilic MMT (OMMT) was prepared by cationic exchange between Na–MMT and CTAB in an aqueous solution. The suspension solution containing 12.5 g of Na–MMT and 4.6 g of CTAB was mixed in 240 mL of distilled water. The suspension solution was stirred at 75°C for 2 h, and the exchanged Na–MMT was filtered

Correspondence to: Y.-E Fang (fye@ustc.edu.cn).

Journal of Applied Polymer Science, Vol. 90, 1692–1696 (2003)

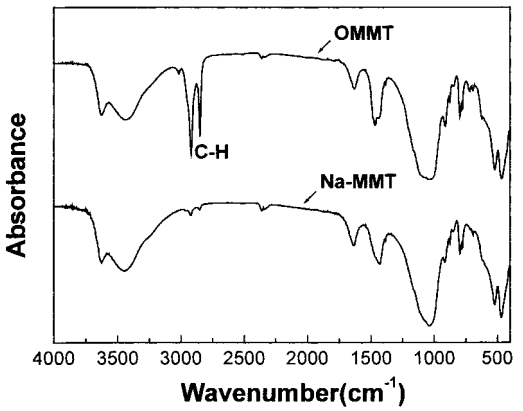

Figure 1 FTIR spectra of OMMT and Na–MMT.

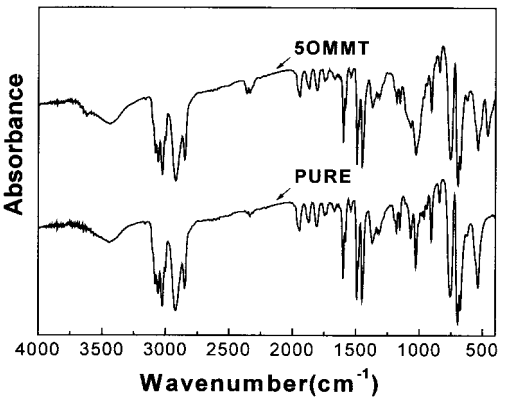

Figure 2 FTIR spectra of pure PS and PS/MMT nanocomposites.

and washed with distilled water until no bromide ion is detected with 0.1*M* $AgNO_3$ solution. The product was then dried in a vacuum oven at 60°C for 12 h. The OMMT was obtained and then ground with a mortar, and sieved by a 280-mesh Cu grid. The overall CTAB content in the OMMT was about 22 wt % [by thermal gravimetric analysis (TGA)].

Synthesis of PS/MMT nanocomposites

The desired amount of the OMMT was dispersed in styrene monomer by ultrasonication at room temperature for 15 min to obtain suspensions. The suspension solution was added in reactor vessels and bubbled with N_2 gas (99.5%) to remove oxygen, after which the polymerization was carried out in a 2.22 $\times$ 10^{15} Bq ^{60}Co γ-ray source with 90-kGy radiation dose and 65 Gy/min radiation dose rate at room temperature. After drying under vacuum for 24 h at 80°C, the product was obtained.

Characterization

IR spectra were recorded on a Bruker Vector-22 FTIR spectrometer (Bruker Instruments, Billerica, MA), scanning from 4000 to 400 cm^{-1} at room temperature. The samples were ground with KBr crystal and that mixture was pressed into a flake for IR measurement.

X-ray diffraction was carried out with a Japanese Rigaku D/max γ_A X-ray diffractometer equipped with graphite monochromatized Cu–K_α radiation (λ = 0.154178 nm, 40 kV, 100 mA) and a slit collimator. The scanning range was 1.5–10° with a scanning rate of 2°/min. The diffraction patterns were recorded with a scintillation counter at 25°C. The distance between the sample and the detector was 185 mm.

The microstructure of nanocomposites was imaged using a JEOL 2010 EX (Tokyo, Japan) high-resolution transmission electron microscopy (HRTEM). The samples for HRTEM were cut to 60-nm-thick sections with a diamond knife.

Differential scanning calorimetry (DSC) was carried out on a Perkin–Elmer Pyrus 1 DSC (Perkin Elmer Cetus Instruments, Norwalk, CT) at a heating rate of 10°C/min under N_2 flow from 40 to 200°C.

TGA was conducted on a Perkin–Elmer Pyrus 1 TGA under N_2 flow from 25 to 550°C at a heating rate of 10°C/min.

RESULTS AND DISCUSSION

Structure of PS/MMT nanocomposites

Clays such as montmorillonites are considered 2 : 1 layered silicates. Their crystal lattice consists of two silica tetrahedral sheets fusing into an octahedral sheet, with a lateral dimension of 200–2000 nm and a thickness of about 1 nm. Isomorphous substitutions of Si^{4+} for Al^{3+} in the tetrahedral lattice and of Al^{3+} for Mg^{2+} in the octahedral sheet can generate negative charges that are counterbalanced by cations such as Ca^{2+} and Na^+. Many cationic surfactants can easily exchange with the hydrated cations between the layers and render the clay more organophilic as a result of the very weak force holding the hydrated cations.

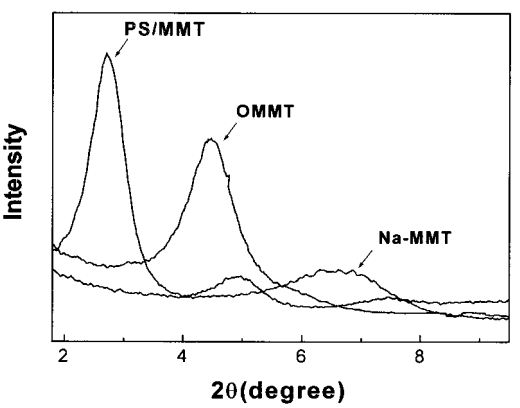

Figure 3 XRD patterns of Na–MMT, OMMT, and PS/MMT nanocomposites.

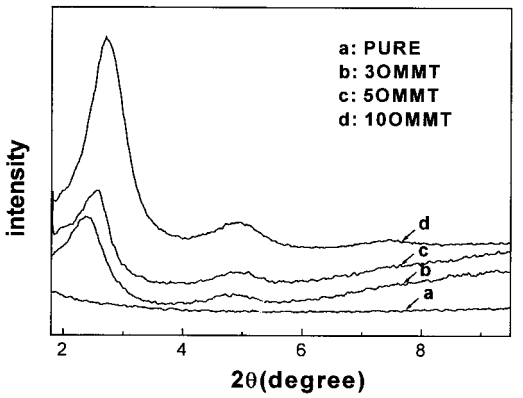

Figure 4 XRD patterns of pure PS and PS/MMT nanocomposites with different OMMT contents.

Because the surface energy of the organophilic clay is much lower, many polymers and monomers can much more easily intercalate between the galleries.

Figure 1 shows the IR spectra of Na^+–MMT and OMMT. The characteristic absorption band of Na^+–MMT is at 1040 cm^{-1}. After being treated by CTAB, the characteristic absorption bands of C—H stretching are shown at 2850 and 2919 cm^{-1}. The representative IR spectra of pure PS and PS/MMT nanocomposites are shown in Figure 2. The absorption bands at 3025 and 2920 cm^{-1} are associated, respectively, with the aromatic C—H stretching and aliphatic C—H stretching of PS. The absorption bands of PS/MMT at 3630, 1040, and those between 600 and 400 cm^{-1} correspond, respectively, to –OH stretching of the lattice water; Si—O stretching and Al—O stretching; and Si—O bending, which are the most distinct bands that are different from those with pure PS. This means PS has been intercalated into the sheets of MMT, a finding that is also supported by Noh and Lee.[20]

Further evidence for the intercalation can be obtained by X-ray diffraction (XRD). Figure 3 shows the wide-angle powder XRD patterns of Na–MMT, OMMT, and PS/MMT nanocomposites. The diffraction pattern of the (001) plane of OMMT occurring at 4.47°, corresponding to 1.97 nm, shifted from that of the Na–MMT (6.65°), which indicates that the CTAB is inserted into the sheets of the OMMT. After intercalation polymerization, the diffraction pattern of PS/MMT nanocomposites is at 2.71° (3.26 nm). Thus CTAB is an effective intercalative reagent, thus making the MMT organophilic and enlarging the spacing between sheets; the styrene monomer can then easily enter between the sheets and polymerize to form intercalative nanocomposites. Figure 4 presents the XRD curves of pure PS and PS/MMT nanocomposites with different OMMT loading contents: 3 wt % (3OMMT); 5 wt % (5OMMT), and 10 wt % (10OMMT). In this figure, pure PS does not exhibit any diffraction peak, but when the amount of the OMMT dispersed in PS is only 3 wt %, there is a much more intensified peak, which indicates that intercalation has occurred. When the amount of OMMT was increased to 10 wt %, there was no distinct shift, indicating that the distance between the sheets of the PS/MMT was not affected by the amount of the OMMT.

In addition to XRD and IR, to validate the morphology of the nanocomposites, the internal nanometer-scale structure was observed by HRTEM, which provides direct visualization of the morphology. Figure 5(a) shows the HRTEM images of the PS/MMT nanocomposites containing 5 wt % OMMT. This is a larger

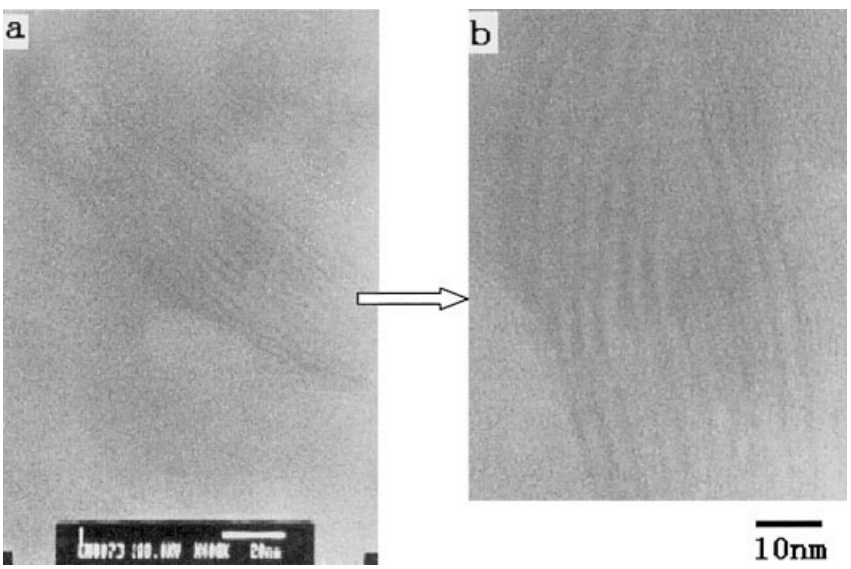

Figure 5 (a) HRTEM of PS/MMT nanocomposites containing 5 wt % OMMT (×400,000, 20-nm scale); (b) enlarged image of the intercalated MMT layers.

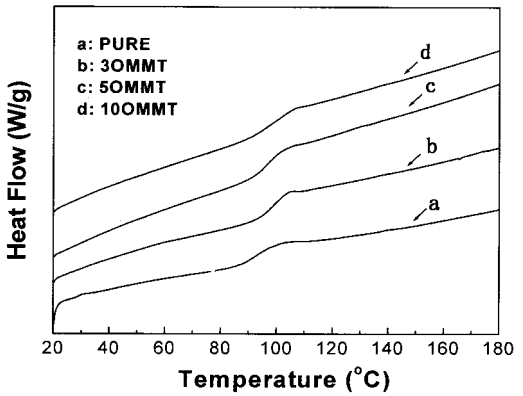

Figure 6 DSC thermograms of pure PS and PS/MMT nanocomposites with different OMMT contents.

intercalated tactoid, which is composed of some parallel clay layers with an average of about 10 layers. These layers show long-range order and can be measured by XRD. There are many similar intercalated tactoids in the nanocomposites. This implies the MMT is not well dispersed in the nanocomposites. Figure 5(b) is the magnified image of Figure 5(a) by about 3 times. The well-ordered layer of the clay (dark lines), alternating with the chains of the PS (white part), can be observed. The spacing between adjacent sheets is about 3.5 nm, which corresponds to what was obtained by XRD measurement. This provides direct evidence that the PS chains have been intercalated into the layers of the MMT and that a PS/MMT nanocomposite has formed.

Thermal properties

Figure 6 shows DSC traces of pure PS and PS/clay nanocomposites. Pure PS has an endotherm at 87°C, corresponding to the glass-transition temperature (T_g) of the PS. All PS/MMT nanocomposites show higher T_g than that of pure PS. When the content of the OMMT is only 3 wt %, the T_g is evidently improved and is attributed to the restriction of the intercalated polymer chains between the sheets of the MMT, which thus prevents the segmental motions of the polymer chains. On the other hand, however, the T_g does not increase with increased amounts of OMMT, thus confirming that the 3 wt % OMMT can effectively improve the T_g of the PS.

TGA thermograms of pure PS and PS/MMT nanocomposites are presented in Figure 7. Evidently at the initial stage of degradation, the thermal degradation temperature of the nanocomposites does not increase with increased contents of OMMT. If we designate onset decomposition temperature at the temperature of 5% weight loss, we find that these nanocomposites have almost the same onset decomposition temperatures as that of pure PS. Only for 5OMMT does its thermal degradation rate become slower than that of pure PS. When the temperature is increased above 410°C, all the nanocomposites have a lower thermal degradation rate than that of pure PS, indicating the enhancement of thermal stability of the nanocomposites. Moreover, their thermal stability is always in the order 10OMMT < 3OMMT < 5OMMT. Compared to PS, cetyltrimethylammonium has a much lower decomposition temperature at about 230°C (by TGA). Furthermore, these nanocomposites are mainly composed of many intercalated tactoids (Fig. 5). The decomposition of the cetyltrimethylammonium part may accelerate the decomposition of the PS chain adjacent to it, which may thus be a possible reason that the thermal degradation rates of 3OMMT and 10OMMT are higher than that of pure PS at the initial stage of thermal decomposition. 5OMMT, however, has good thermal stability, which is possibly because the MMT has better dispersion in 5OMMT than in 3OMMT and 10OMMT, although 5OMMT is also composed of many intercalated tactoids. Thus, the good dispersion of MMT can make up for the effect of the decomposition of the cetyltrimethylammonium part. This is our conjectural mechanism, although further study is still required. With further increases of temperature, because the MMT has an excellent barrier property that prevents permeation of atmospheric air and assists in the formation of char after thermal decomposition, all the nanocomposites have a lower thermal degradation rate than that of pure PS.

CONCLUSIONS

PS/MMT nanocomposites can be successfully prepared by γ-ray radiation polymerization. The intercalative structure of PS/MMT was characterized by XRD and HRTEM. The improvement of the thermal properties is attributed to the fact that PS chains are fixed between layers of the clay and the nanolayers of the clay can effectively check the segmental motions of

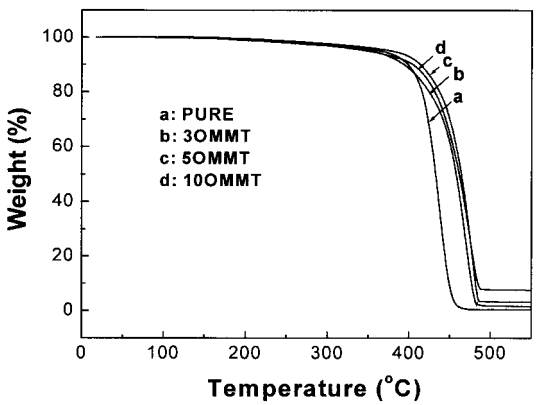

Figure 7 TGA thermograms of pure PS and PS/MMT nanocomposites with different OMMT contents.

the polymer chains, thus imparting an excellent barrier property. When the OMMT content is 3 wt %, the intercalative structure of the PS/MMT nanocomposite can be formed and its thermal property can be quickly obtained.

References

1. Usuki, A.; Kojima, Y.; Kawasumi, M. J Mater Res 1993, 8, 1179.
2. Garces, J. M.; Moll, D. J.; Bicerano, J. Adv Mater 2000, 12, 1835.
3. Gilman, J. W.; Awad, W. H.; Davis, R. D. Chem Mater 2002, 14, 3776.
4. Mark, J. E. Polym Eng Sci 1996, 15, 2905.
5. Frisch, H. L.; Mark, J. E. Chem Mater 1996, 8, 1735.
6. Kojima, Y.; Usuki, A.; Kawasumi, M. J Mater Res 1993, 14, 1185.
7. Lerchner, J.; Seidel, J.; Wolf, G. J Mater Sci 2001, 4, 4567.
8. Usuki, A.; Kawasumi, M.; Kojima, Y. J Mater Res 1993, 8, 1174.
9. Vaia, R. A.; Jandt, K. D.; Kramer, E. J. Macromolecules 1995, 28, 8080.
10. Usuki, A.; Kato, M.; Okada, A. J Appl Polym Sci 1997, 63, 137.
11. Chen, T. K.; Tien, Y. I.; Wei, K. H. J Polym Sci Part A: Polym Chem 1999, 37, 2225.
12. Harris, D. J.; Bonagamba, T. J.; Schmidt-Rohr, K. Macromolecules 1999, 32, 6718.
13. Liu, X. H.; Wu, Q. J.; Berglund, L. A. Polymer 2001, 42, 8235.
14. Tyan., H. L.; Liu, Y. C.; Wei, K. H. Chem Mater 1999, 11, 1942.
15. Chen, K. H.; Yang, S. M. J Appl Polym Sci 2002, 86, 414 (2002).
16. Pluta, M.; Galeski, A.; Alexandre, M. J Appl Polym Sci 2002, 86, 1497.
17. LeBaron, P. C.; Pinnavaia, T. J. Chem Mater 2001, 13, 3760.
18. Chen, Z.; Gong, K. J Appl Polym Sci 2002, 84, 1499.
19. Rhodes, C. M.; Brown, D. R. Clay Miner 1994, 29, 799.
20. Noh, M. W.; Lee, D. C. Polym Bull 1999, 42, 619.